Chapter 3

Recombinant BCG Expressing ESX-1 of *Mycobacterium marinum* Combines Low Virulence with Cytosolic Immune Signalling and Improved TB Protection

Cell Reports. Volume 18, Issue 11, Pages 2752-2765 (March 2017)

by Matthias I. Gröschel[1,2], Fadel Sayes[1], Sung Jae Shin[3], Wafa Frigui[1], Alexandre Pawlik[1], Mickael Orgeur[1], Robin Canetti[1], Nadine Honoré[1], Roxane Simeone[1], Tjip S. van der Werf[2], Wilbert Bitter[4], Sang-Nae Cho[3],Laleh Majlessi[1] and Roland Brosch[1].

[1] Unit for Integrated Mycobacterial Pathogenomics, Institut Pasteur, Paris, France
[2] Department of Pulmonary Diseases and Tuberculosis, University Medical Center Groningen, Groningen, The Netherlands
[3] Department of Microbiology, Institute for Immunology and Immunological Diseases, Yonsei University College of Medicine, Seoul, South Korea
[4] Department of Medical Microbiology and Infection Control, VU University Medical Center, Amsterdam, The Netherlands

Abstract

Recent insights into the mechanisms by which *Mycobacterium tuberculosis*, the etiologic agent of human tuberculosis, is recognised by cytosolic nucleotide sensors have opened new avenues for rational vaccine design. The only licensed anti-tuberculosis vaccine, *Mycobacterium bovis* BCG, provides limited protection. A feature of BCG is the partial deletion of the ESX-1 type VII secretion system, which governs phagosomal rupture and cytosolic pattern recognition, key intracellular phenotypes linked to increased immune signalling. Here, by heterologously expressing the *esx-1* region of *Mycobacterium marinum* in BCG, we engineered a low-virulence, ESX-1-proficient, recombinant BCG (BCG::ESX-1 *Mmar*) that induces the cGas/STING/TBK1/IRF-3/type I interferon axis and enhances AIM2 and NLRP3 inflammasome activity, resulting in both higher proportions of $CD8^+$ T cell effectors against mycobacterial antigens shared with BCG and polyfunctional $CD4^+$ Th1 cells specific to ESX-1 antigens. Importantly, independent mouse vaccination models show that BCG::ESX-1 *Mmar* confers superior protection relative to parental BCG against challenges with highly virulent *M. tuberculosis*.

3.1 Introduction

Tuberculosis (TB) is a chronic infectious disease caused by *Mycobacterium tuberculosis* that continues to be among the top five causes of death in 18 countries[1]. Increased prevention would be a tremendous asset in controlling the global epidemic, as reflected by World Health Organization's new End TB Strategy[2]. Rational design of an improved vaccine that is able to prevent active disease would be the most effective mea- sure in TB control[3]. Thus, numerous efforts are being undertaken to develop improved anti-TB vaccines, some of which have recently entered clinical development[4,5].

The currently licensed anti-TB vaccine *Mycobacterium bovis* BCG, also known as Bacille Calmette Guérin, confers insufficient protection against pulmonary TB in adolescents and adults[6]. The absence of a 9.5-kb genomic region across all BCG strains, termed Region of Difference 1 (RD1), is the principal molecular determinant underlying BCG attenuation[7,8]. RD1 harbours genes required for the paradigm type VII secretion (T7S) ESX-1, or ESAT-6 secretion system that is dedicated to the export of proteins that play key roles in host-pathogen interactions and pathogenic potential[9]. During infection of host phagocytes, a functional ESX-1 secretion system and selected lipids (i.e., phthiocerol dimycocerosates) are required for communication of *M. tuberculosis* with the host cytosol[10,11], with subsequent detection of bacterial DNA by cytosolic sensors, and mitochondrial stress[12]. This process leads to a cascade of innate immune signalling events[13-15], including reinforced AIM-2 (Absence in Melanoma 2) and NLRP3 inflammasome activation, increased interleukin-1β (IL-1β) and/or IL-18 secretion[16-18] and activation of the cyclic GMP-AMP synthase (cGas)/Stimulator of Interferon Genes (STING)/TANK-binding kinase 1 (TBK1)/IRF3 axis. The latter signalling cascade results in the production of type I interferons (IFNs)[19]. Apart from innate immune activation, secreted ESX-1 effectors also induce specific host Th1 cell responses with strong protective potential[20,21]. Early attempts to improve the protective efficacy of BCG by heterologously expressing ESX-1 from *M. tuberculosis*, a biosafety level (BSL) 3 organism, produced mixed results. Vaccine efficacy was improved[22], but as a side effect virulence was increased[7], making this recombinant BCG strain likely too virulent as to be used for vaccine applications. Thus, the rationale emerged to express the ESX-1 systems of related but less pathogenic mycobacteria in BCG. *M. tuberculosis* H37Rv and *M. marinum*, a BSL2 aquatic mycobacterium that can infect fish or frogs and occasionally causes skin infections in humans, share a substantial core genome, with high amino acid sequence conservation, particularly across the genes encoding the ESX-1 system (Figure 3.1A). Here, we engineered a recombinant BCG candidate vaccine that harboured the *esx-1* locus of *M. marinum* (BCG::ESX-1 *Mtb*). We then interrogated the biological and immunological consequences of this heterologous ESX-1 *Mmar* expression in the context of vaccination. Using different

murine infection models, we identified previously undiscovered immunological features of recombinant BCG linked to cytosolic pattern recognition and we provide compelling evidence of significantly improved protective vaccine efficacy.

3.2 Results

Construction of the Recombinant BCG ESX-1 *Mmar* Proficient Strain

An *esx-1* locus-containing clone was selected from a Bacterial Artificial Chromosome (BAC) library of *M. marinum* reference strain M. This library was originally constructed to scaffold and validate the whole-genome sequence assembly of this strain[23]. The BAC clone was used as substrate for subcloning a 38.7-kb-sized fragment into the integrating cosmid vector pYUB412[24] (Figures 3.1A and B). Sequence analysis revealed that the cloned fragment carried a nucleotide deletion in the *eccCb1* gene (6 C instead of 7 C in the published genome sequence[23] GenBank CP000854 at position 6589,378-84) (Figure 3.8), causing a frameshift in *EccCb1*. Further analysis showed that the same *eccCb1* nucleotide deletion was present in the genome of the M strain (MPasteur), used for construction of the BAC library (Figure 3.8). This finding likely explains the previously reported differences in ESAT-6 secretion and virulence between the attenuated *M. marinum* MVU variant and other *M. marinum* M variants used in diverse laboratories[25-28], as the *M. marinum* MVU also harbours this mutation. The frameshift in the cosmid was repaired using a phage lambda Red recombineering approach[29]. We then transformed the ESX-1-repaired cosmid into BCG Pasteur 1173P2 (Figure 3.1C). Comparison of the in vitro growth characteristics of the obtained recombinant BCG::ESX-1 *Mmar* strain showed that they were similar to other BCG strains (Figure 3.9A).

The Heterologous ESX-1 System Is Functional in BCG::ESX-1 *Mmar*

The main secreted *M. tuberculosis* ESX-1 effectors ESAT-6 and CFP-10 share very high amino acid sequence identity with their *M. marinum* orthologs (Figure 3.9B), so we assessed the functionality of the heterologous ESX-1Mmar secretion machinery by using major histocompatibility complex (MHC)-II-restricted T cell hybridomas specific to different ESX-1 effectors. In this model, presentation of ESX-1 effectors is dependent on their proper secretion[30]. BCG::ESX-1 *Mmar*-infected bone-marrow-derived dendritic cells (BM-DCs) presented ESAT-6Mmar and CFP-10Mmar to specific T cell hybridomas in a manner indistinguishable from BCG::ESX-1 *Mtb*-infected BM-DCs (Figure 3.1D). Similarly, EspC (Rv3615c), an ESX-1- secretion-associated protein that forms secretion-needle-like structures[31,32], and is exported in

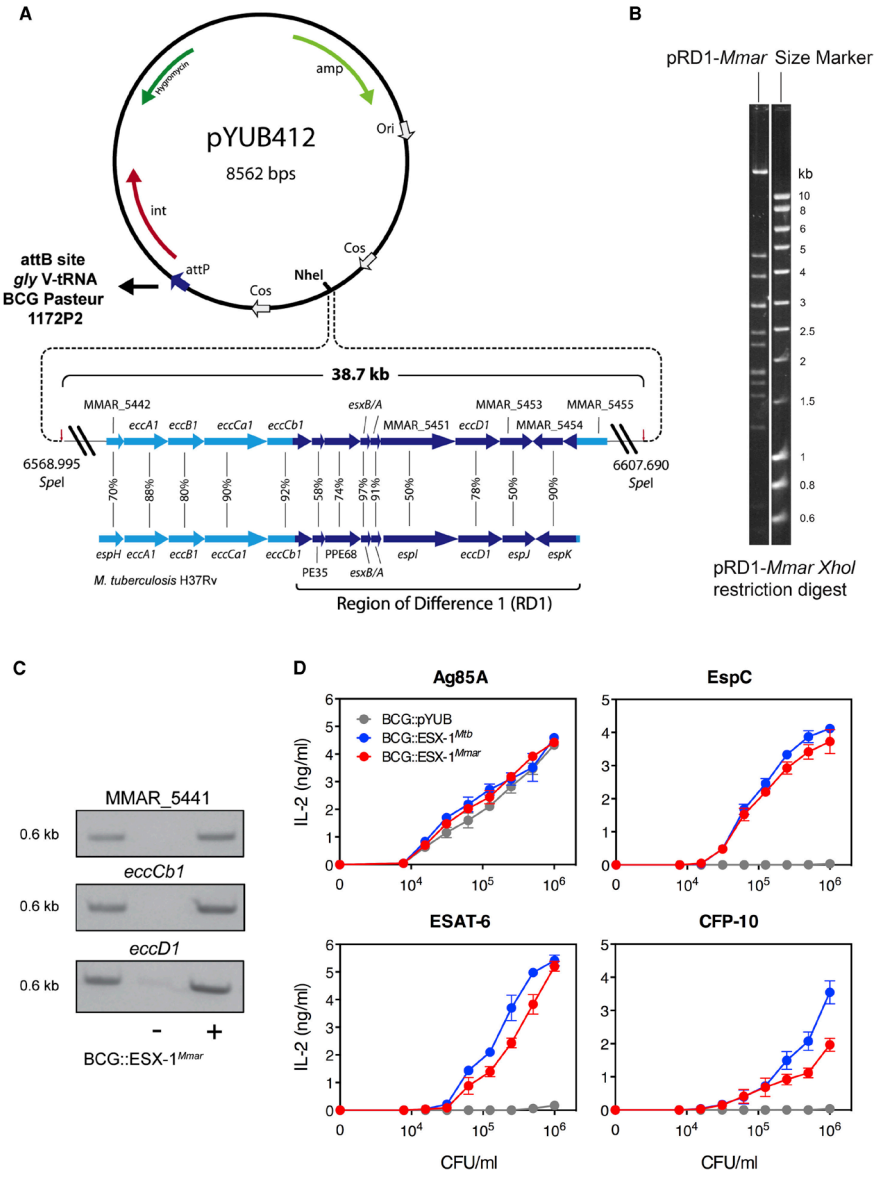

Figure 3.1: Stable Genetic Complementation of BCG Pasteur Integrating the *esx-1* Region of *M. marinum*. *(Legend continued on the following page)*

Figure 3.1: *Cont'd:*

(A) Schematic representation of the integrating vector[24], the NheI cloning site, and the 38.7-kb insert from *M. marinum* M containing the *esx-1* locus. Amino acid sequence identities between gene products in the orthologous *esx-1* loci of *M. marinum* and *M. tuberculosis* are depicted in percentages.

(B) Ethidium-bromid stained fragments of XhoI restriction digest of pRD1-Mmar, separated by agarose gel electrophoresis.

(C) PCR-based verification of the integration of the *esx-1* locus into BCG::ESX-1 *Mmar*, using several primers spanning the *esx-1* locus of *M. marinum* and negative and positive DNA controls.

(D) Demonstration of secretion of different ESX-1 substrates by BCG::ESX-1 *Mmar* strain through antigenic presentation by infected phagocytes. MHC-II-restricted antigenic presentation of ESAT-6, EspC and CFP-10 by BM-DCs generated from C57BL/6 (H-2^b) or C3H (H-2^k) mice, infected in vitro by different BCG strains, to T cell hybridomas; NB11 (specific to ESAT-6:1-20, restricted by I-A^b), IF1 (specific to EspC:40-54, restricted by I-A^b) or XE12 (specific to CFP-10:11-25, restricted by I-A^k), respectively. In this assay, the efficacy of antigenic presentation, evaluated by T cell activation and IL-2 production, is proportional to the amounts of ESX-1 secreted substrate. The DE10 hybridoma (specific to Ag85A:241-260, restricted by I-A^b) was used as a positive control. Error bars represent SD. The results are representative at least of two independent experiments.

a co-dependent way with ESAT-6[33], was efficiently presented by BM-DCs infected with either BCG::ESX-1 *Mmar* and BCG::ESX-1 *Mtb* (Figure 3.1D). All tested BCG strains induced the antigenic presentation of the control antigen Ag85A, secreted by the Twin-Arginine Translocation (TAT) pathway (Figure 3.1D). These data confirmed the functionality of the heterologous *M. marinum* ESX-1 system in BCG::ESX-1 *Mmar*, including the successful interaction with the transacting EspACD proteins of BCG that are encoded outside the cosmid-contained *M. marinum* fragment.

BCG::ESX-1 *Mmar* Shows Reduced Virulence Compared to BCG::ESX-1 *Mtb*

We next compared in vivo growth in severe combined immunodeficient (SCID) mice of BCG::ESX-1 *Mmar* with *M. tuberculosis* H37Rv, BCG::ESX-1 *Mtb* and parental BCG Pasteur. In this model in which weight loss is an index of disease development, BCG::ESX-1 *Mmar* induced a weight-loss curve similar to BCG Pasteur (Figures 3.2A and B). In contrast, mice infected with *M. tuberculosis* H37Rv or BCG::ESX-1 *Mtb* lost 20% of their weight significantly earlier, indicating that BCG::ESX-1 *Mmar* is more attenuated than BCG::ESX-1 *Mtb*[7,22].

BCG::ESX-1 *Mmar* Modulates the Host Innate Immune Response via Phagosomal Rupture

To determine further ESX-1 Mmar-associated biological consequences, we first confirmed that BCG::ESX-1 *Mmar* induced phenotypic and functional maturation of DC in a similar manner as control strains (BCG::pYUB, BCG::ESX-1 *Mtb* and wild-type (WT) *M. tuberculosis* H37Rv). This effect was evaluated by the upregulation of the CD40, CD80, and CD86 co-stimulatory molecules, modulation of MHC-I/II expression (Figure 3.10A), and production of pro/anti-inflammatory cytokines and chemokines (Figure 3.10B). As selected ESX-1-proficient mycobacteria such as *M. marinum*, *M. kansasii*, or *M. tuberculosis*[28,34,35] have been shown to induce ESX-1- mediated phagosome-to-cytosol communication, we explored whether BCG::ESX-1 *Mmar* was able to induce phagosomal rupture in host phagocytes. We used a flow-cytometric fluorescence resonance energy transfer (FRET) approach based on a green-to-blue fluorescence shift following cleavage of cytosolic coumarin-cephalosporin-fluorescein 4 (CCF4) by endogenous mycobacterial β-lactamase[10]. Analysis of infected human THP-1 macrophages revealed that BCG::ESX-1 *Mmar* induced a solid blue shift, implying contact with the host cytosol, albeit to a lesser degree compared to *M. tuberculosis* H37Rv and BCG::ESX-1 *Mtb* (Figure 3.3A). In contrast, the ESX-1-deficient negative control BCG strain did not induce a blue shift in the infected cells (Figure 3.3A).

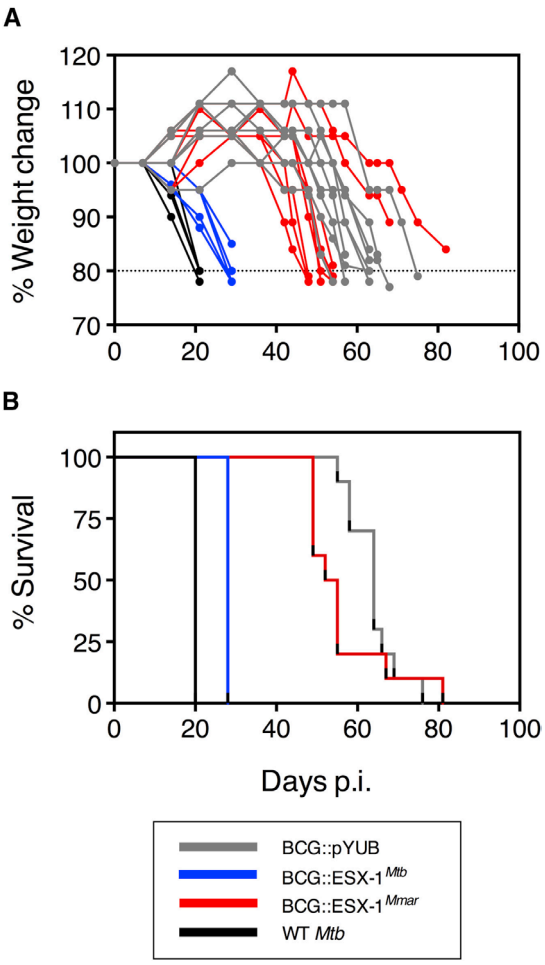

Figure 3.2: **Attenuated Virulence of BCG::ESX-1 *Mmar* Strain, as Evaluated in Immunocompromised Mice.** SCID mice (n = 10 per group) were infected intravenously (i.v.) with 1 x 10^6 colony-forming units (CFUs)/mouse of different recombinant BCG strains in order to monitor the percentage of their weight change **(A)** and the survival **(B)** compared to *M. tuberculosis* H37Rv (WT *Mtb*). Mice were killed when reaching the humane endpoint, defined as the loss of >20% of bodyweight. The obtained median survival times for groups of SCID mice were the following: *Mtb* WT 20 d; BCG::ESX-1 *Mtb* 28 days; BCG::ESX-1 *Mmar* 53.5 days; BCG Pasteur 64 days. Statistical analyses using the log-rank (Mantel-Cox) test showed that the differences in survival between groups of animals infected with BCG::ESX-1 *Mmar* and *Mtb* WT or BCG::ESX-1 *Mtb* were highly statistically significant ($p < 0.0001$), whereas for BCG::ESX-1 *Mmar* versus BCG Pasteur no significant difference was obtained ($p = 0.2136$). In contrast, median survival times for BCG::ESX-1 *Mtb* versus BCG Pasteur were highly statistically significant

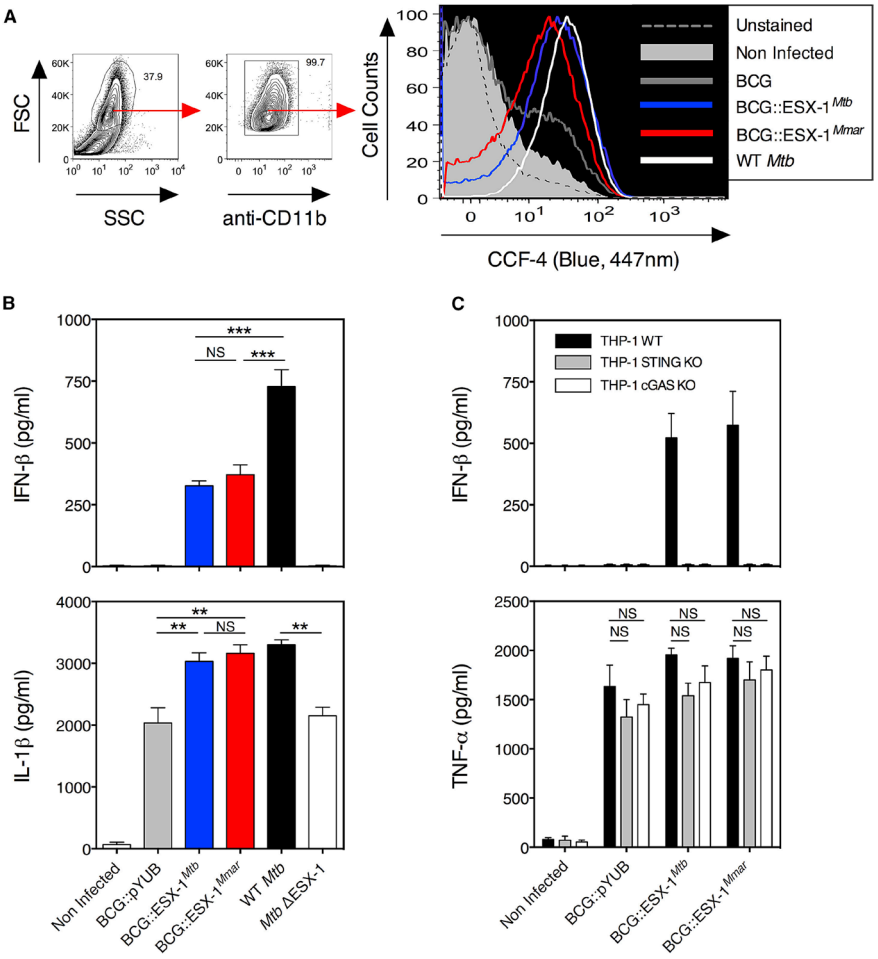

Figure 3.3: Dynamic Effects of Functional ESX-1 Secretion System of BCG::ESX-1 *Mmar* on the Host Innate Immune Responses. *(Legend continued on the following page)*

Figure 3.3: *Cont'd:*

(A) Gating strategy and results of phagosomal rupture assay in WT THP-1 human macrophages, infected with different recombinant BCG strains, as detected at day 3 post-infection by CCF-4 FRET-based cytometry, compared to controls.
(B and C) ELISA-based quantification of IFN-β and IL-1β (B), or IFN-β and TNF-α **(C)** contents in the culture supernatants of the infected WT or mutant THP-1 cells at 24 hr post-infection. The results are representative of two independent experiments. NS, not significant, ** or ***, statistically significant, as determined by one-way ANOVA test with Tukey's correction, with $p < 0.005$ or $p < 0.001$, respectively. Error bars indicate SD levels.

Infection of WT THP-1 macrophage-like cells with BCG:: ESX-1Mmar or control strains showed that BCG::ESX-1 *Mmar* and BCG::ESX-1 *Mtb* both induced IFN-β production, although at a lower level than WT *M. tuberculosis*. In comparison, IFN-β secretion was not detected in BCG::pYUB and *M. tuberculosis* ΔESX-1 (Figure 3.3B). Infection of THP-1 cells deficient in either cGAS or STING, revealed that neither BCG nor *M. tuberculosis* (either WT or recombinant) led to IFN-β release (Figure 3.3C). As a functional control, we showed that cGAS or STING-deficient THP-1 cells released tumour necrosis factor-α (TNF-α)-like WT (Figure 3.3C). These data support our contention that a type I IFN response by ESX-1-proficient BCG strains depends on cytosolic exposure of mycobacterial DNA to then associate with cGAS.

In parallel, we found that infection with BCG::ESX-1 *Mmar*, BCG::ESX-1 *Mtb* or WT *M. tuberculosis*, significantly enhanced release of active IL-1β, compared to BCG::pYUB and *M. tuberculosis* ΔESX-1 (Figure 3.3A). These data are in agreement with earlier studies, which revealed that the release of active IL-1β is partially dependent on the interaction of mycobacterial DNA with AIM2[36].

Since ESX-1-dependent activation of STING has been reported to increase autophagy[37], we tested whether the BCG::ESX-1 *Mmar* or BCG::ESX-1 *Mtb* increased the presence of the cytosolic autophagy effector microtubule-associated protein 1A/1B-light chain 3 (LC3)-II. Using a flow-cytometry-based assay, we observed increased LC3-II accumulation in THP-1 cells infected with ESX-1-proficient recombinant BCGs relative to BCG::pYUB-infected cells (Figure 3.11A), without notable differences in cell mortality (Figure 3.11B). However, the observed differences between BCG WT and recombinant strains remained relatively small, in concordance with previous studies using western blotting or confocal microscopy[37,38] (Figure

3.11A).

BCG::ESX-1 *Mmar* Induces Potent Polyfunctional Th1 Cell Responses against ESX-1-Secreted Antigens

Protection against TB largely depends on the host's ability to generate potent Th1 cell responses against mycobacterial protective antigens[39]. C57BL/6 (H-2b) or C3H (H-2k) mice, immunised subcutaneously (s.c.) with BCG::ESX-1Mmar, mounted IFN-g T cell responses against *esx-1*-encoded ESAT-6 and CFP-10 antigens as well as ESX-1-secretion-associated EspC (Figures 3.12). These responses were similar to those detected in the BCG::ESX-1 *Mtb*- or WT *M. tuberculosis*-immunised groups. BCG::ESX-1 *Mmar*-immunised mice also displayed IFN-γ T cell responses against non-ESX-1-associated antigens shared with BCG that were comparable to those induced by the BCG::pYUB control, as exemplified by Ag85A-, PE19-, or PPE25-specific IFN-γ release (Figure 3.12A).

In-depth characterisation of the functional Th1 subsets by intracellular cytokine staining (ICS) (Figures 3.4A, 3.13, and 3.14) showed that BCG::ESX-1 *Mmar*, BCG::ESX-1 *Mtb*, as well as BCG::pYUB, all induced comparable percentages of Th1 cytokine-producing cells and similar compositions in single-, double-, and triple-Th1 cytokine producing cells, specific to the antigens present in BCG, i.e., Ag85A (Figure 3.11B) and PE19 or PPE25 (Figure 3.14A). In addition, BCG::ESX-1 *Mmar* and BCG::ESX-1 *Mtb* induced similar ESAT-6 or EspC-specific Th1 responses (Figure 3.4B). Indeed, the total percentage of Th1 cytokine-producing cells per mouse against these antigens was comparable among the mice immunised with the two ESX-1-proficient recombinant BCG strains (Figure 3.14). The responses were dominated by IL-2+ TNF-α+ and TNF-α+ IFN-γ+ double-positive and IL-2+ TNF-α+ IFN-γ+ triple-positive $CD4^+$ T cells. Furthermore, the amount of Th1 cytokines produced by ESAT-6 specific $CD4^+$ T cell subsets in response to BCG::ESX-1 *Mmar* and BCG::ESX-1 *Mtb* were comparable (Figure 3.4C).

BCG::ESX-1 *Mmar* Boosts Initiation of Anti-Mycobacterial Host $CD8^+$ T Cell Immunity

Independent lines of evidence point to a major role of $CD8^+$ T cells in anti-mycobacterial protection[40,41]. To evaluate the impact of BCG complementation with ESX-1, we immunised C3H (H-2k) mice that specifically recognise a MHC-I-restricted CFP-10:32-39 epitope[42] and found that the mice mounted $CD8^+$ T cell responses against CFP-10, as detected by IFN-γ production subsequent to stimulation of splenocytes with the peptide (Figure 3.5A). In addition, higher percentages of TNF-α+ IFN-γ+ bi-functional $CD8^+$ T cells specific to Ag85A:144-152[43], TB10.4:20-28[44], or PPE26: 44-

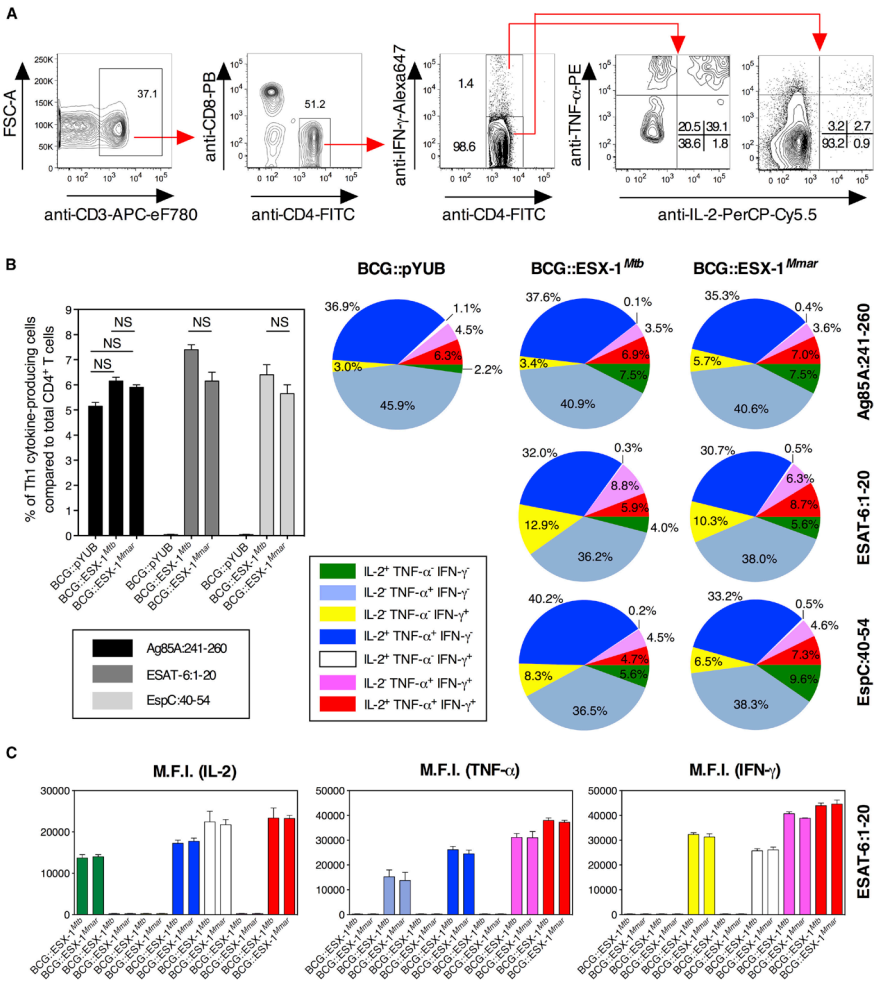

Figure 3.4: Dissection of Th1 Cell Responses Induced by BCG::ESX-1 *Mmar* Immunisation. *(Legend continued on the following page)*

Figure 3.4: *Cont'd:*

(A) Gating strategy adopted to detect different functional subsets of specific Th1 effectors in the spleen of BCG::ESX-1 *Mmar*-immunised C57BL/6 mice using ICS. Cytometric plots represent 5% contours, representative of three mice per group. Shown are cultures of splenocytes stimulated by ESAT-6:1-20.

(B) Percentages of antigen-specific Th1 cytokine producing T cells compared to total $CD4^+$ T splenocytes (left) and composition of Th1 cytokine-producing functional $CD4^+$ T cells, specific to different mycobacterial antigens, at 28 days post-immunization. Total splenocytes from each group were stimulated in vitro with 10 μg/mL of different synthetic peptides containing I-A^b-restricted immunodominant epitopes, prior to ICS, in order to determine frequencies of single-, double-, or triple-positive $CD4^+$ cells producing IL-2, TNF-α, and/or IFN-γ. NS, not significant as determined by one-way ANOVA test with Tukey's correction.

(C) The geometric mean fluorescence intensities (MFIs), proportional to the intracellular amounts of IL-2, TNF-α, or IFN-γ, in each of the ESAT-6-specific functional Th1 subsets, as determined in the spleen of mice immunised with BCG::ESX-1 *Mmar* or BCG::ESX-1 *Mtb*. Additional information is provided in Figures 3.13 and 3.14.

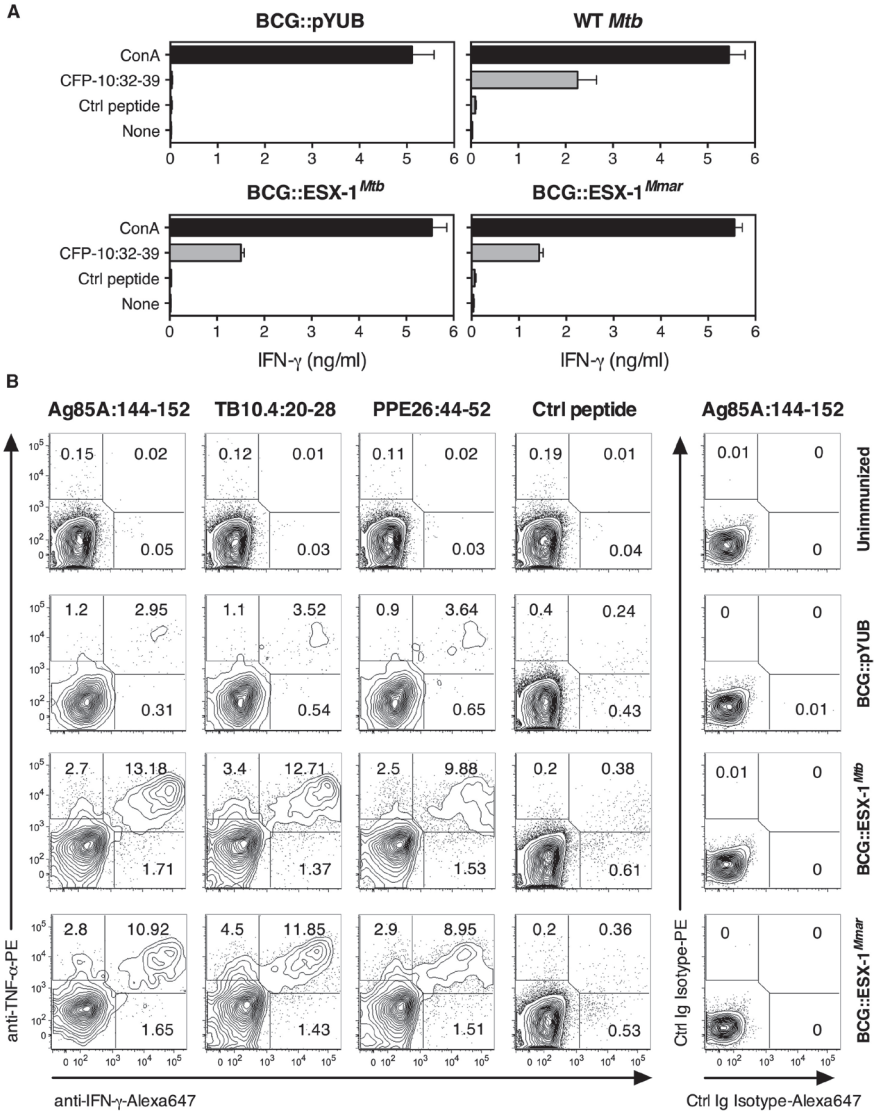

Figure 3.5: Enhanced Induction of Key CD8⁺ T Cell Effectors by BCG::ESX-1 *Mmar* in Immunocompetent Mice. *(Legend continued on the following page)*

Figure 3.5: *Cont'd:*

(A)T cell IFN-γ responses of C3H (H-2^k) mice (n = 3 per group) immunised s.c. with 1 x 10^6 CFUs/mouse of different BCG strains, as assessed at 4 weeks post-immunisation. Pool of total splenocytes of the immunised mice were stimulated in vitro with synthetic MHC-I-restricted CFP-10-derived peptides during 72 hr. Error bars represent SD.

(B) Detection of TNF-α- and/or IFN-γ-producing $CD3^+$ $CD4^-$ $CD8^+$ T splenocytes by ICS applied on total splenocytes of BALB/c (H-2^d) mice (n = 3 per group), immunised s.c. with 1 x 10^6 CFUs/mouse of different BCG strains. At 5 weeks post-immunisation, splenocytes were stimulated in vitro with MHC-I H-$2K^d$-restricted epitopes from Ag85A, TB10.4, PPE26, or the LCMV-NP:118-126 as a negative control peptide. In parallel, stimulated cells were stained with control immunoglobulin (Ig) isotypes. Cytometric plots represent 5% contours with outliers, representative of three mice per group. The results are representative of two independent experiments.

52-[45] MHC-I-restricted epitope were detected in the spleen of BCG::ESX-1 *Mmar*- or BCG::ESX-1 *Mtb*-immunised BALB/c (H-2d) mice, relative to their BCG-immunised counterparts (Figure 3.5A). The increase in $CD8^+$ T cell responses against non-ESX-1-secreted antigens upon immunisation with ESX-1-proficient BCGs supports the notion that ESX-1-mediated phagosomal rupture facilitates cross-presentation of mycobacterial antigens either due to type I IFN production[46] or by enhanced access of antigens to the cytosolic presentation machinery[47]. The potentially increased persistence of ESX-1-proficient BCGs in the vaccinated host may also contribute to sustained availability of mycobacterial antigens required for the initiation of robust $CD8^+$ T cell effectors[48].

BCG::ESX-1 *Mmar* Protects Mice from TB Better than Standard BCG Vaccines

To assess the protective efficacy of the BCG::ESX-1 *Mmar* as a potential vaccine candidate, we immunised s.c. groups of C57BL/6 mice (n = 5 per group) with the different BCG strains. After 4 weeks, mice were challenged with *M. tuberculosis* H37Rv via the aerosol route and mycobacterial loads were determined in lungs and spleen 4 weeks later (Figure 3.6A). Both BCG ESX-1-proficient strains were superior to BCG Danish 1331, the model control BCG strain used in TB vaccine research, or BCG::pYUB in protecting against an *M. tuberculosis* H37Rv challenge both in the lungs and in spleen

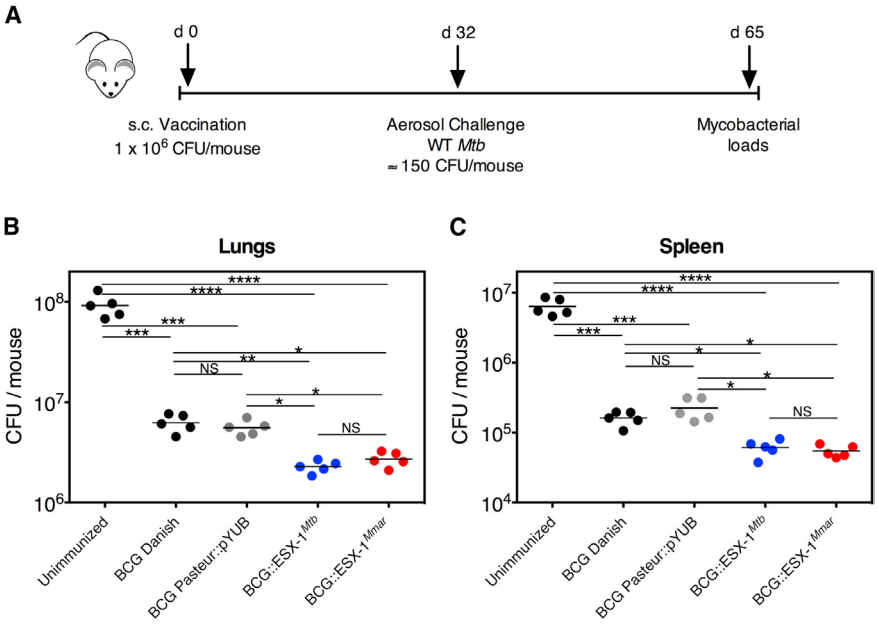

Figure 3.6: Improved Protection Potential of BCG::ESX-1Mmar Strain Significantly Enhances Protective Capacity against an *M. tuberculosis* H37Rv Challenge in Mice.

(A) Immunisation protocol of mice adopted in order to evaluate protective capacity of different BCG strains.

(B and C) C57BL/6 mice (n = 5 per group) were left unimmunised or vaccinated s.c. with 1 x 10^6 CFUs/mouse of BCG Pasteur::pYUB, BCG Danish, BCG::ESX-1 *Mtb* or BCG::ESX-1 *Mmar* strain with ca. 150 CFUs/mouse of *M. tuberculosis* H37Rv strain via aerosol route, as determined by CFU counting in the lungs day 1 post-infection. The mycobacterial loads in the lungs (B) and spleen (C) of individual mice were determined. NS, not significant, *, **, ***, ****, statistically significant, as determined by one-way ANOVA test with Tukey's correction, with $p < 0.05$, $p < 0.005$, $p < 0.001$, or $p < 0.0001$, respectively.

(Figures 3.6B and C) in this model. These data suggest that BCG::ESX-1 *Mmar* and BCG::ESX-1 *Mtb* show similar protective efficacies that are, in turn, superior to the parental BCG strains.

To further explore its protective performance, BCG::ESX-1 *Mmar* was tested in an independent preclinical vaccine trial within the framework of the TBVAC2020 consortium, where potential TB vaccine candidates are compared head-to-head relative to BCG Danish 1331 (Figure 3.7A). BCG::ESX-1 *Mmar* showed significantly enhanced protection against a challenge with the highly virulent *M. tuberculosis* strain HN878 (Beijing family) (Figure 3.7B) and *M. tuberculosis* strain M2 from the Harleem family (Figure 7C), as evidenced by greatly reduced mycobacterial loads in the lungs and spleen, as well as decreased proportions of inflamed lung tissue (Figure 3.7D).

3.3 Discussion

With millions of doses delivered across generations of humans around the world, BCG is perhaps the most well-known example of a live, attenuated vaccine and is still widely used today as no higher-performing alternatives have been licensed to date. Developed in the 1920s by Calmette and Guérin after longterm in vitro passaging of a virulent *Mycobacterium bovis* isolate that became irreversibly attenuated, vaccination with BCG of an estimated 3 billion individuals confirmed that BCG was safe in the immunocompetent host[49]. Besides BCG, the other human anti-TB vaccine used at a larger scale is the vole-bacillus *Mycobacterium microti*. Different attenuated variants were successfully used to vaccinate 10,000 adolescents in the UK[50] and half a million babies in the former Czechoslovakia[51] in the 1960s.

However, reflection on the history of almost 100 years of human anti-TB vaccination shows that despite undeniable beneficial effects conferred to small children, vaccination with BCG or *M. microti* has been insufficient to prevent the current global re-emergence of TB. Interestingly, BCG and *M. microti* strains have one major genetic feature in common. They have independently deleted portions of the region of difference 1 (RD1) [52,53], which in M. tuberculosis and many other mycobacteria encodes the ESX-1 type VII secretion system[9,54,55]. The biological basis for key ESX-1-mediated effects are primarily linked to the ESX-1-dependent induction of phagosome-cytosol communication[28,47,56]. Indeed, mycobacterial cytosolic contact triggers a cascade of cellular signalling events that are of upmost importance for innate and adaptive immune responses. ESX-1-deficient BCG and *M. microti* vaccine strains are unable to initiate these responses[9,39,57].

We reasoned that influencing phagosome biology through ESX-1 secretion might enhance the protective ability of BCG, and we wanted to uncouple the beneficial immunological ESX-1-mediated effects from the gain-of-virulence linked to the insertion of genes from a BSL3 organism

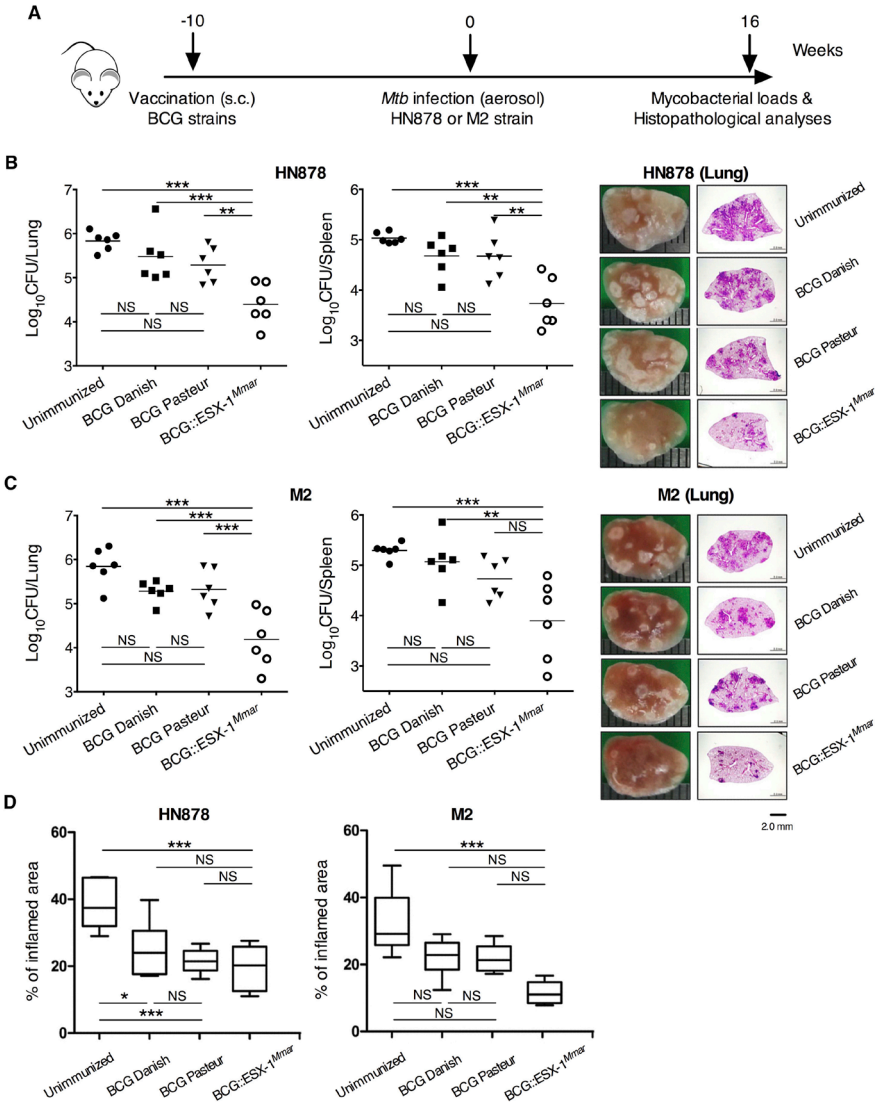

Figure 3.7: Improved Protection Potential of BCG::ESX-1 *Mmar* Strain Relative to Standard BCG Strains in Mice against a Challenge with Hypervirulent *M. tuberculosis* Strains HN878 and M2. *(Legend continued on the following page)*

Figure 3.7: *Cont'd:*

(A) Immunisation protocol with different BCG strains

(B and C) Bacterial loads in the lungs and spleens 26 weeks post-immunisation and 16 weeks after aerosol challenge with the *M. tuberculosis* HN878 (B) or M2 (C) strains. Mice were challenged with the *M. tuberculosis* HN878 strain (approximately 200 CFUs/mouse) or M2 strain (approximately 50–60 CFUs/mouse) via the aerosol route. The CFUs in the lungs and spleens of each group were analysed by culturing lung and spleen homogenates and enumerating the bacteria. Note that CFU data shown correspond to counts that were obtained from the left-superior lobes of the lungs. The data are presented as the median $\pm$ interquartile range (IQR) $\log_{10}$ CFUs/organ (n = 6), and the levels of significance for comparisons between samples were determined by a one-way ANOVA, followed by Dunnett's multiple comparison test.

(D) Lung samples collected for histopathology were preserved overnight in 10% normal buffered formalin, embedded with paraffin, sliced into 4- to 5-μm-thick sections, and stained with H&E. The superior lobes of the right lung were stained with H&E to assess the severity of inflammation. The level of inflammation in the lungs was evaluated using ImageJ software (NIH). Percentages of the inflamed areas are presented as whisker boxplots (whiskers represent minimum and maximum values) (n = 6), and a one-way ANOVA followed by Dunnett's test was used to determine the significance of the findings.

into BCG. We thus heterologously expressed in BCG the ESX-1 from *M. marinum*, a mycobacterium that shares with BCG the BSL2 classification. Successful integration of the *M. marinum* ESX-1 locus was confirmed by PCR and use of a panel of ESX-1 antigen- specific T cell hybridomas. Interestingly, we detected lower antigenic presentation of CFP-10 by dendritic cells infected with BCG::ESX-1 *Mmar* compared to BCG::ESX-1 *Mtb*, which might reflect a lower CFP-10 antigen availability due to the heterologous expression of *M. marinum* proteins that need to cooperate for secretion with proteins from BCG.

The introduction of the ESX-1 *Mmar* region into BCG resulted in a minor, non-significant increase in virulence relative to parental BCG Pasteur and was greatly reduced compared to the virulence of BCG::ESX-1 *Mtb*. As the magnitude of phagosomal rupture by BCG::ESX-1 *Mmar* and BCG::ESX-1 *Mtb* was comparable, it suggests that phagosome escape is not the only determining factor that explains the virulence differences observed between ESX-1-proficient and ESX-1-deficient mycobacteria. Alternatively, the heterologous expression of a large DNA fragment from a more distantly related species with different host specificity, i.e., *M. marinum*, in BCG might reduce the in vivo fitness of the recombinant BCG::ESX-1 *Mmar*, although we observed similar in vitro growth characteristics to standard BCG.

We next evaluated the immunological repercussions of the ESX-1 introduction into BCG by analyzing innate immune responses, particularly in light of the most recent literature. IL-1β is protective in the context of *M. tuberculosis* infection[58], and its catalytic cleavage is mediated by the NLRP3 inflammasome/caspase-1 pathway[59]. We showed that ESX-1-proficient BCGs mount a higher IL-1β response suggesting that cytosolic access of mycobacterial compounds promotes activation of the inflammasome. In addition to induction of IL-1β, recent evidence points to a role for ESX-1-mediated cytosolic contact in NLRP3-inflammasome- mediated secretion of IL-18 by infected CD11c+ immune cells[17]. This leads to non-cognate production of IFN-γ by *M. tuberculosis*-antigen-independent memory $CD8^+$ T cells and NK cells. Such IL-18-dependent and rapid IFN-γ responses are not induced by current anti-TB vaccines[17,60]. In this context, the rationale is strengthened for leveraging ESX-1 function as an important additional element in the design of third-generation vaccines and host-directed therapy against TB.

By acquiring cytosolic access, mycobacterial molecular fingerprints, such as extracellular DNA, can also be sensed by germline-encoded pattern recognition receptors in host cell such as AIM2[36,61] or cGAS[13-15]. We observed that the BCG::ESX-1 strains induced IFN-β mediated by the cGAS/STING pathway in human macrophages. We acknowledge that the role of type I IFNs in the context of *M. tuberculosis* infection is somewhat conflicted[62]. Studies in humans[63] and in animal models report a detrimental role of type I IFNs during *M. tuberculosis* infection[19,64]. A possible explanation is that

IFN-α/β undermine inflammasome activation and associated host protective cytokines such as IL-1β[65]. However, this pro-bacterial role of type I IFNs during infection with *M. tuberculosis* could turn out to be pro-host during vaccination. While type I IFNs negatively regulate active IL-1β secretion during *M. tuberculosis* infection[66], we observed both increased IL-1β and IFN-β production induced by the ESX-1-proficient BCG vaccine candidates. Therefore, if an activated cGas/STING/TBK1/IFR3/ type I IFN pathway contributes to the persistence of attenuated vaccine strains and the activation of non-infected neighboring cells[67], this effect might favorably increase the spatial and temporal interplay between the vaccine and the host immune system, ultimately contributing to improved vaccine efficacy.

Apart from the prompt innate immune response, the late adaptive immune system plays a key role in anti-mycobacterial immunity[68]. We found that the BCG::ESX-1 *Mmar* induces a potent Th1 cell response against strong immunogens exported by ESX-1, which enlarges the antigenic repertoire compared to the currently used BCG vaccine, and thus represents a desirable feature in the light of the incomplete protection conferred by BCG. The presence of polyfunctional Th1 cytokine-producing cells against ESX-1-secreted antigens upon vaccination with the recombinant BCGs adds another convincing feature of the broadened T cell specificities. Apart from $CD4^+$ T cells, we detected improved $CD8^+$ T cell responses by analysing functional $CD8^+$ T cells. This strong adaptive immune response could be partly explained by a bridging function of activated IFN-β between innate and adaptive immunity, as has been described for type I IFNs[46]. Importantly, in addition to type I IFNs IL-1β and inflammasome activation also play roles in regulating the differentiation and function of $CD8^+$ T cells during *M. tuberculosis* infection[69]. $CD8^+$ T cell effectors are primed through increased inflammasome signalling (IL-1β), in concert with the up-regulation of chemo-attractants CCL2, CCL5, and CXCL10, of which we detected elevated levels (Figure 3.10B) [46,70]. These data support a model where ESX-1- mediated cytosolic access assists presentation to and activation of the cytosolic presentation machinery through induction of type I IFNs[46] and potentially increased bacterial persistence[48].

The hypothesis that ESX-1-mediated cytosolic access improves the performance of recombinant BCG through enhanced innate immune signalling and enlarged antigenic repertoire is supported by our results from the mouse models where BCG::ESX-1 *Mmar* showed superior protective efficacy compared to parental BCG. These results are in accord with those obtained using an attenuated *M. tuberculosis* strain that lacks the characteristic *esx-5*-associated *pe/ppe* genes, but harbours all other components of the ESX-5 system, as well as an intact ESX-1 system[45]. Like BCG::ESX-1 *Mmar*, this strain named *Mtb*Δ*ppe25-pe19* is able to induce innate immune responses linked to cytosolic pattern recognition and shows significantly improved

protection against an *M. tuberculosis* challenge in a mouse infection model[71]. These results suggest that, despite the different genetic background and the different origin of the ESX-1 system, ESX-1-mediated functions are essential for increasing protection levels above those provided by vaccination with standard BCG strains.

In conclusion, the heterologous expression of an *M. marinum* derived ESX-1 system in BCG yielded a recombinant vaccine candidate with relatively low virulence levels in SCID mice, which are comparable with those of other BCG strains72, and a capacity to induce selected innate and adaptive immune responses that depend on phagosome-cytosol communication in the host phagocyte. Such responses are not induced by first-generation anti-TB vaccines such as BCG or M. microti and might as well not be induced by the second-generation anti-TB vaccine candidates that have recently entered clinical development[17]. Given that 90%–95% of M. tuberculosis exposed individuals do not develop active TB disease during their lifetime, host immune effectors are largely capable of inducing protective immunity[73]. We propose that a virulence-attenuated, ESX-1- proficient BCG vaccine might be best able to mimic the natural route of infection and induce the "correct" phagosomal biology, leading to protective immunity at the same points of host-pathogen contact as *M. tuberculosis*. We argue that this important biological feature should not be left out from the rational design of third-generation vaccines, giving BCG::ESX-1 *Mmar* a clear potential to better control TB.

3.4 Experimental Procedures

Mycobacterial strains

Mycobacterial strains were grown in Dubos broth medium complemented with Albumine, Dextrose and Catalse (ADC, Difco, Becton Dickinson, Le Pont-de-Claix, France) and hygromycin 50 μg/ml. The mycobacterial concentrations were determined by OD 600nm measurement and CFU counting on Middlebrook 7H11 solid Agar medium complemented with Oleic acid, Albumine, Dextrose and Catalse (OADC, Difco, Becton Dickinson) after 16-18 days of incubation at 37°C. The two challenge *M. tuberculosis* strains HN878 and M2 were obtained from the strain collections of the International Tuberculosis Research Center (ITRC, Changwon, Gyeongsangnam-do, Korea).

Preparation and reparation of cosmid DNA

The genetic construct containing the ESX-1 region of *M. marinum* in the integrating cosmid vector pYUB412 was obtained by subcloning a 38.7 kb-sized SpeI fragment from a clone of an *M. marinum* M strain BAC library[23]

into the unique NheI site of integrating cosmid vector pYUB412[24]. Repair of a frameshift mutation in the cosmid was undertaken using a phage lambda Red-based approach, as described[29]. Selection of the repaired clone was facilitated by the temporary introduction of an apramycin cassette into the *esx-1* locus next to the repaired nucleotide, which required a synonymous codon change for creating an SpeI restriction site. After sequence verification, cosmid DNA was freshly prepared from a strain of recombinant *Escherichia coli* DH10B (Invitrogen Corporation, Cergy Pontoise, France) that contained the repaired cosmid. *M. bovis* BCG Pasteur 1173P2, held at Institut Pasteur, was grown at 37°C on Middlebrook 7H11 medium (Difco) supplemented with OADC. To obtain electrocompetent cells, bacteria from solid culture were transferred into 7H9 medium complemented with ADC and grown for 10 days. Cells were harvested and washed twice with H2O and once with 10% Glycerol at RT. The pellet was resuspended in 2 ml of 10% glycerol. The cell suspension was mixed with the integrative ESX-1 cosmids and electroporated using a Bio-Rad gene pulser XCell (Marnes-la-Coquette, France) at 2500 mVolt. Electroporated cells were cultured overnight at 37°C and then plated on 7H11 medium containing hygromycin 50 μg/ml. Antibiotic resistant colonies were collected after 3 weeks and analysed for the presence of the integrated cosmid.

Antigen presenting assay

Several MHC-II-restricted T-cell hybridomas specific to mycobacterial antigens were used in order to detect the secretion by mycobacteria, which leads to the antigenic presentation by the infected BM-DC of different ESX-1 substrates, as follows: I-Ab-restricted NB11 (specific to ESAT-6:1-20) [21,30]. IF1 (specific to EspC:40-54) and I-Ak-restricted XE12 (specific to CFP-10:11-25) [74]. DE10 T-cell hybridoma (specific to Ag85A:241-260) [21] were used as an ESX-1-independent control antigen. BM-DCs were obtained from femurs of 8-10-week-old female C57BL/6JRj (H-2b) or C3H/HeJ (H-2k) mice (Janvier, Le Genest-Saint-Isle, France), depending on the MHC restriction of the T-cell epitopes to be studied and as described previously[45]. BM-DCs plated at 2 x 10^5 cells/well in flat-bottom, 96-well culture plates in completed, antibiotic-free RPMI 1640. Four hours later, BM-DCs were infected with various M.O.I of mycobacteria. After overnight incubation, the infected DCs were washed twice prior to the addition of 1 x 10^5 cells per well of the T-cell hybridomas of interest in 100 μl. After over-night incubation, specific IL-2 produced by T-cell hybridomas was quantified in the co-culture supernatants using ELISA.

ELISA and Multiplex cytokine/chemokine assays

Levels of IL-1α, IL-1β, TNF-α, IL-6, IL-10, IL-12p70, MCP-1 (CCL2), RANTES (CCL5), IP-10 (CXCL10) in the BM-DC culture supernatants were determined by multiple ProcartaPlex (Affymetrix) kit assays according to the manufacturer's protocol and a Luminex X-100 Reader. For ELISA experiments, monoclonal antibodies (mAbs) specific to murine IL-2 or IFN-γ were purchased from BD Pharmingen (Le pont-de-Claix, France). Murine TNF-α-specific mAbs were obtained from eBioscience (Paris, France). Human IL-1β and IFN-β were quantified using the DY201-05 (R&D Systems) and 41410 (PBL Assay Science) kits, respectively.

FRET assay by flow cytometry

The principle of the β-lactamase CCF-4 assay has recently been described10. In short, human pro-monocytic THP-1 cells were plated in 24-well plate at 5 x 10^5 cells/well in 2 ml of RPMI complemented with 10% FCS, in the presence of 20 ng/ml of PMA (Pharbol 12-myristate 13-acetate, Sigma Aldrich) for 72h. Upon 2h incubation with different mycobacterial strains at an multiplicity of infection (M.O.I.) of 1, cells were washed three times with PBS. Fresh medium was added and cells were incubated for 4 days. After staining with anti-CD11b-APC (BD Pharmingen) and CCF-4 (Invitrogen), cells were analysed on a CyAn cytometer system (Beckman Coulter, Villepinte, France). Phagosomal rupture was observed once the CCF-4 signal switched from green (535 nm) to blue (447nm), when CCF-4 was not cleaved the signal remained green.

Intracellular detection of LC3-II

PMA-differentiated THP-1 cells plated in 12-well plates at 1 x 106 per well were infected at an M.O.I. of 10 with the different mycobacterial strains. At 6h post-infection, cells were washed and stained with APC-anti-CD11b mAb. Next, permeabilisation and intracellular staining with FITC-anti-LC3-II mAb was performed by use of a Millipore (Temecula, CA, USA) autophagy detection reagent pack according to the manufacturer's instructions.

Immunogenicity and T-cell assay

For immunological studies 6-8-week-old female C3H and C57BL/6 mice (Janvier) were immunised s.c. with 1 x 10^6 CFU of the mycobacterial strains in 200 μl PBS, as previously described[45]. After 3-4 weeks, splenocytes from each group were cultured on 96 well plates (1 x 10^6 cells/well) using 2mM GlutaMax complemented HL-1 medium (Biowhittaker, Lonza, France) in

the presence of various mycobacterial antigens. After 72h of incubation IFN-γ was quantified in culture supernatants using ELISA.

T-cell intracellular Th1 cytokine assay

Splenocytes of immunised C57BL/6 mice (n = 2-3 mice per group) were cultured in 24 wells plate at 1 x 10^7 cells/well. Cells were stimulated with 10 μg/ml of different peptides in the presence of 1 μg/ml anti-CD28 (clone 37.51) and 1 μg/ml of anti-CD49d (clone 9C10-MFR4.B) mAbs (BD Pharmingen) during 12-14h at 37°C 5% CO2. Upon 3h of incubation with Golgi Plug (Brefeldin A, BD Pharmingen), cells were harvested and stained with appropriate dilutions of AlloPhycoCyanin (APC)-eFluor780-anti-CD3ε, FITC-anti-CD4 and/or PB-anti-CD8α mAbs (BD Pharmingen) at 4°C in dark. To perform the ICS assay the surface stained cells were permeabilized using Cytofix/Cytoperm (BD Pharmingen) and incubated with appropriate dilutions of PerCP-Cyanine5.5-anti-IL-2 (clone JES6-5H4, eBioscience), PE-anti-TNF-α (clone 554419, BD Pharmingen) and Alexa Fluor647-anti-IFN-γ (clone XMG1.2, eBioscience) mAbs or appropriate Ig isotypes during 30 minutes at 4°C. Finally, cells were washed twice in PermWash buffer followed by FACS buffer (PBS containing 3% Fetal Bovin Serum and 0.1% NaN3) and then fixed with 4% PFA overnight at 4°C. The stained cells (1 x 10^6/sample) were acquired in an LSR Fortessa flow cytometer system by use of BD FACS Diva software (BD Bioscience).

In vivo experiments

Studies in immunocompetent and immunodeficient mice were performed according to European and French guidelines (Directive 86/609/CEE and Decree 87–848 of 19 October 1987) after approval by the Institut Pasteur Safety, Animal Care and Use Committee (Protocol 11.245) and local ethical committees (CETEA 2012–0005 and CETEA 2013–0036). For virulence studies six-week-old female SCID mice (Janvier) were infected intravenously with 200 μl of 5 x 10^6 bacteria/mouse, and the survival of mice was monitored. The humane endpoint was defined as loss of ¿20% of bodyweight. Sample size choice was determined by taking into account the rule of 3Rs (replacement, reduction, refinement) and statistical requirements.

For protection experiments using *M. tuberculosis* H37Rv as challenge, six week-old female C57BL/6 mice were left unvaccinated or were immunised s.c. with 1 x 10^6 CFU per mouse with the different BCG strains. One month later, mice were challenged with ca. 150 CFU of virulent *M. tuberculosis* H37Rv WT strain per mouse by use of a homemade nebuliser via aerosol route of infection as described[45]. CFU counts in the lungs of the challenged mice were determined at day one. Four weeks post infection, mice were sacrificed and CFU in lungs and spleen were determined.

For protection experiments using challenges with clinical *M. tuberculosis* strains HN878 or M2, specific pathogen-free female C57BL/6N at 6 weeks of age were purchased from Japan SLC, Inc. (Shijuoka, Japan) and were maintained under barrier conditions in a BL-3 biohazard animal facility at the Yonsei University Medical Research Center in an environment with a constant temperature (24±1°C) and humidity (50±5%). The animals were fed a sterile commercial mouse diet and were provided with water ad libitum under standardised light-controlled conditions (12-h light and dark periods). The mice were monitored daily, and none of the mice exhibited any clinical symptoms or illness during the experimental period.

BCG-vaccinated groups were subcutaneously immunised one time with $2.0x10^5$ CFU of each BCG strain. To study the protective efficacy of the vaccine strains, mice were challenged 11 to 12 days post infection with strains HN878 or M2. Briefly, the mice were exposed to a predetermined dose of the *M. tuberculosis* HN878 or M2 strain for 60 min in the inhalation chamber of an airborne infection apparatus (Glas-Col, Terre Haute, IN, USA) to expose the mice to approximately 200 CFU of viable *Mtb*. At 16 weeks post-challenge, mice were killed and numbers of viable bacteria in the lungs and the spleens of the mice were evaluated. Briefly, the bacterial count in each organ was determined by plating organ homogenates on Middlebrook 7H11 agar (Becton Dickinson, Franklin Lakes, NJ, USA) supplemented with 10% OADC enrichment medium until the late exponential phase. CFU counts were performed after 4 weeks of incubation at 37°C. Lung samples collected for histopathology were preserved overnight in 10% normal buffered formalin, embedded with paraffin, sliced into 4- to 5-mm-thick sections, and stained with hematoxylin-eosin (H&E). The superior lobes of the right lung were stained with H&E to assess the severity of inflammation. The level of inflammation in the lungs was evaluated using ImageJ software (National Institutes of Health, USA).

All animal studies involving *M. tuberculosis* HN878 and M2 challenges were performed in accordance with Korean Food and Drug Administration (KFDA) guidelines. The experimental protocols used in this study were reviewed and approved by the Ethics Committee and Institutional Animal Care and Use Committee (Permit Number: 2015-0274) of the Laboratory Animal Research Center at Yonsei University College of Medicine (Seoul, Korea).

Statistical Analyses

GraphPad Prism software (GraphPad Software, La Jolla, CA) was used to perform statistical analyses. The One Way ANOVA test with Tukey's correction was employed to analyse the obtained data with multiple comparisons. For protection experiments using *M. tuberculosis* strains HN878 and M2, data in the graphs are expressed as the means ± standard devi-

ation. The data from the in vivo experiments are reported as the medians $\pm$ interquartile range (IQR). The significance of differences between two groups was determined using unpaired Student's t-tests or the significance of differences between three or more groups was evaluated with one-way ANOVA followed by Dunnett's multiple comparison test using statistical software (GraphPad Prism Software, version 5.01; San Diego, CA, USA). *p < 0.05, **p < 0.01 and ***p < 0.001 were considered statistically significant.

Accession numbers

The accession number for selected flow-cytometric data reported in this paper is Flow Repository: FR-FCM-Zy24 (https://flowrepository.org/id/FR-FCM-ZY24)

Acknowledgments

We thank Veit Hornung (University of Munich) for kindly providing cGAS and STING K.O. cell lines; Peter Sebo (Czech Academy of Sciences, Prague) for ESAT-6 and CFP-10 proteins, Jean-Marc Ghigo for vector pKOBEG and advice, and Lalita Ramakrishnan, Thierry Soldati, and Timothy Stinear for *M. marinum* M strains. We are also grateful to Timothy Stinear for critically reading of the manuscript and advice. M.I.G. receives an MD/PhD scholarship and support from the Graduate School of Medical Sciences, both University of Groningen, the Netherlands. This study was in part supported by the European Union's Horizon 2020 Research and Innovation Program (grant 643381 TBVAC2020), the Agence National de Recherche (grants ANR-14-JAMR- 001-02, ANR-14-CE-08-0017-04, ANR-10-LABX-62-IBEID), the Fondation pour la Recherche Médicale FRM (DEQ20130326471), and the Institut Pasteur (PTR441). This study was also supported by the International Research & Development Program through the National Research Foundation of Korea (NRF) funded by the Ministry of Science, ICT & Future Planning of Korea (NRF-2014K1A3A7A03075054). The mycobacterial construct BCG::ESX-1 *Mmar* has been patented under number PCT/-EP2015/062457.

3.5 References

1. GBD 2013 Mortality and Causes of Death Collaborators. Global, regional, and national age-sex specific all-cause and cause-specific mortality for 240 causes of death, 1990-2013: a systematic analysis for the Global Burden of Disease Study 2013. Lancet 385, 117–171 (2015).

2. Uplekar, M. et al. WHO's new end TB strategy. Lancet 385, 1799–1801 (2015).

3. Knight, G. M. et al. Impact and cost-effectiveness of new tuberculosis vaccines in low- and middle-income countries. Proc. Natl. Acad. Sci. U. S. A. 111, 15520–15525 (2014).

4. Fletcher, H. A. et al. T-cell activation is an immune correlate of risk in BCG vaccinated infants. Nat. Commun. 7, 11290 (2016).

5. Grode, L. et al. Safety and immunogenicity of the recombinant BCG vaccine VPM1002 in a phase 1 open-label randomized clinical trial. Vaccine 31, 1340–1348 (2013).

6. Kaufmann, S. H. E., Evans, T. G. & Hanekom, W. A. Tuberculosis vaccines: time for a global strategy. Sci. Transl. Med. 7, 276fs8 (2015).

7. Pym, A. S., Brodin, P., Brosch, R., Huerre, M. & Cole, S. T. Loss of RD1 contributed to the attenuation of the live tuberculosis vaccines Mycobacterium bovis BCG and Mycobacterium microti. Mol. Microbiol. 46, 709–717 (2002).

8. Hsu, T. et al. The primary mechanism of attenuation of bacillus Calmette–Guérin is a loss of secreted lytic function required for invasion of lung interstitial tissue. Proc. Natl. Acad. Sci. U. S. A. 100, 12420–12425 (2003).

9. Gröschel, M. I., Sayes, F., Simeone, R., Majlessi, L. & Brosch, R. ESX secretion systems: mycobacterial evolution to counter host immunity. Nat. Rev. Microbiol. 14, 677–691 (2016).

10. Simeone, R. et al. Cytosolic access of Mycobacterium tuberculosis: critical impact of phagosomal acidification control and demonstration of occurrence in vivo. PLoS Pathog. 11, e1004650 (2015).

11. Augenstreich, J. et al. ESX-1 and phthiocerol dimycocerosates of Mycobacterium tuberculosis act in concert to cause phagosomal rupture and host cell apoptosis. Cell. Microbiol. 19, (2017).

12. Wiens, K. E. & Ernst, J. D. The Mechanism for Type I Interferon Induction by Mycobacterium tuberculosis is Bacterial Strain-Dependent. PLoS Pathog. 12, e1005809 (2016).

13. Watson, R. O. et al. The Cytosolic Sensor cGAS Detects Mycobacterium tuberculosis DNA to Induce Type I Interferons and Activate Autophagy. Cell Host Microbe 17, 811–819 (2015).

14. Collins, A. C. et al. Cyclic GMP-AMP Synthase Is an Innate Immune DNA Sensor for Mycobacterium tuberculosis. Cell Host Microbe 17, 820–828 (2015).

15. Wassermann, R. et al. Mycobacterium tuberculosis Differentially Activates cGAS- and Inflammasome-Dependent Intracellular Immune Responses through ESX-1. Cell Host Microbe 17, 799–810 (2015).

16. Dorhoi, A. et al. Activation of the NLRP3 inflammasome by Mycobacterium tuberculosis is uncoupled from susceptibility to active tuberculosis. Eur. J. Immunol. 42, 374–384 (2012).

17. Kupz, A. et al. ESAT-6-dependent cytosolic pattern recognition drives noncognate tuberculosis control in vivo. J. Clin. Invest. 126, 2109–2122 (2016).

18. Wong, K.-W. & Jacobs, W. R., Jr. Critical role for NLRP3 in necrotic death triggered by Mycobacterium tuberculosis. Cell. Microbiol. 13, 1371–1384 (2011).

19. Stanley, S. A., Johndrow, J. E., Manzanillo, P. & Cox, J. S. The Type I IFN response to infection with Mycobacterium tuberculosis requires ESX-1-mediated secretion and contributes to pathogenesis. J. Immunol. 178, 3143–3152 (2007).

20. Brodin, P., Majlessi, L., Brosch, R. & Smith, D. Enhanced protection against tuberculosis by vaccination with recombinant Mycobacterium microti vaccine that induces T cell immunity against region of difference 1 antigens. J Inf Dis (2004).

21. Brodin, P. et al. Dissection of ESAT-6 system 1 of Mycobacterium tuberculosis and impact on immunogenicity and virulence. Infect. Immun. 74, 88–98 (2006).

22. Pym, A. S. et al. Recombinant BCG exporting ESAT-6 confers enhanced protection against tuberculosis. Nat. Med. 9, 533–539 (2003).

23. Stinear, T. P. et al. Insights from the complete genome sequence of Mycobacterium marinum on the evolution of Mycobacterium tuberculosis. Genome Res. 18, 729–741 (2008).

24. Bange, F. C., Collins, F. M. & Jacobs, W. R., Jr. Survival of mice infected with Mycobacterium smegmatis containing large DNA fragments from Mycobacterium tuberculosis. Tuber. Lung Dis. 79, 171–180 (1999).

25. Abdallah, A. M. et al. PPE and PE_PGRS proteins of Mycobacterium marinum are transported via the type VII secretion system ESX-5. Mol. Microbiol. 73, 329–340 (2009).

26. Hagedorn, M., Rohde, K. H., Russell, D. G. & Soldati, T. Infection by tubercular mycobacteria is spread by nonlytic ejection from their amoeba hosts. Science 323, 1729–1733 (2009).

27. Ramakrishnan, L., Federspiel, N. A. & Falkow, S. Granuloma-Specific Expression of Mycobacterium Virulence Proteins from the Glycine-Rich PE-PGRS Family. Science 288, 1436–1439 (2000).

28. Simeone, R. et al. Phagosomal rupture by Mycobacterium tuberculosis results in toxicity and host cell death. PLoS Pathog. 8, e1002507 (2012).

29. Chaveroche, M.-K., Ghigo, J.-M. & d'Enfert, C. A rapid method for efficient gene replacement in the filamentous fungus Aspergillus nidulans. Nucleic Acids Res. 28, e97–e97 (2000).

30. Frigui, W. et al. Control of M. tuberculosis ESAT-6 secretion and specific T cell recognition by PhoP. PLoS Pathog. 4, e33 (2008).

31. Ates, L. S. & Brosch, R. Discovery of the type VII ESX-1 secretion needle? Mol. Microbiol. 103, 7–12 (2017).

32. Lou, Y., Rybniker, J., Sala, C. &Cole, S. T. E sp C forms a filamentous structure in the cell envelope of M ycobacterium tuberculosis and impacts ESX-1 secretion. Mol. Microbiol. 103, 26–38 (2017).

33. MacGurn, J. A., Raghavan, S., Stanley, S. A. & Cox, J. S. A non-RD1 gene cluster is required for Snm secretion in Mycobacterium tuberculosis. Mol. Microbiol. 57, 1653–1663 (2005).

34. Stamm, L. M. et al. Mycobacterium marinum escapes from phagosomes and is propelled by actin-based motility. J. Exp. Med. 198, 1361–1368 (2003).

35. Wang, J. et al. Insights on the emergence of Mycobacterium tuberculosis from the analysis of Mycobacterium kansasii. Genome Biol. Evol. 7, 856–870 (2015).

36. Saiga, H. et al. The Recombinant BCG ΔureC::hly Vaccine Targets the AIM2 Inflammasome to Induce Autophagy and Inflammation. J. Infect. Dis. 211, 1831–1841 (2015).

37. Watson, R. O., Manzanillo, P. S. & Cox, J. S. Extracellular M. tuberculosis DNA targets bacteria for autophagy by activating the host DNA-sensing pathway. Cell 150, 803–815 (2012).

38. Romagnoli, A. et al. ESX-1 dependent impairment of autophagic flux by Mycobacterium tuberculosis in human dendritic cells. Autophagy 8, 1357–1370 (2012).

39. Majlessi, L., Prados-Rosales, R., Casadevall, A. & Brosch, R. Release of mycobacterial antigens. Immunol. Rev. 264, 25–45 (2015).

40. Behar, S. M. Antigen-Specific CD8+ T Cells and Protective Immunity to Tuberculosis. in The New Paradigm of Immunity to Tuberculosis (ed. Divangahi, M.) 141–163 (Springer New York, 2013).

41. Ryan, A. A. et al. Antigen load governs the differential priming of CD8 T cells in response to the bacille Calmette Guerin vaccine or Mycobacterium tuberculosis infection. J. Immunol. 182, 7172–7177 (2009).

42. Kamath, A. B. et al. Cytolytic CD8+ T cells recognizing CFP10 are recruited to the lung after Mycobacterium tuberculosis infection. J. Exp. Med. 200, 1479–1489 (2004).

43. Denis, O. et al. Vaccination with plasmid DNA encoding mycobacterial antigen 85A stimulates a CD4+ and CD8+ T-cell epitopic repertoire broader than that stimulated by Mycobacterium tuberculosis H37Rv infection. Infect. Immun. 66, 1527–1533 (1998).

44. Majlessi, L., Rojas, M.-J., Brodin, P. & Leclerc, C. CD8+-T-Cell Responses of Mycobacterium-Infected Mice to a Newly Identified Major Histocompatibility Complex Class I-Restricted Epitope Shared by Proteins of the ESAT-6 Family. Infect. Immun. 71, 7173–7177 (2003).

45. Sayes, F. et al. Strong immunogenicity and cross-reactivity of Mycobacterium tuberculosis ESX-5 type VII secretion: encoded PE-PPE proteins predicts vaccine potential. Cell Host Microbe 11, 352–363 (2012).

46. Le Bon, A. et al. Cross-priming of CD8+ T cells stimulated by virus-induced type I interferon. Nat. Immunol. 4, 1009–1015 (2003).

47. van der Wel, N. et al. M. tuberculosis and M. leprae translocate from the phagolysosome to the cytosol in myeloid cells. Cell 129, 1287–1298 (2007).

48. Woodworth, J. S., Fortune, S. M. & Behar, S. M. Bacterial protein secretion is required for priming of CD8+ T cells specific for the Mycobacterium tuberculosis antigen CFP10. Infect. Immun. 76, 4199–4205 (2008).

49. Fine, P. E. M. et al. Issues relating to the use of BCG in immunization programmes: a discussion document. (Geneva: World Health Organization, 1999).

50. Hart, P. D. & Sutherland, I. BCG and vole bacillus vaccines in the prevention of tuberculosis in adolescence and early adult life. Br. Med. J. 2, 293–295 (1977).

51. Sola, L., Radkovsky, J. & Others. Protective effects of M. microti vaccine against tuberculosis. J. Hyg. Epidemiol. Microbiol. Immunol. 20, 1–6 (1976).

52. Mahairas, G. G., Sabo, P. J., Hickey, M. J., Singh, D. C. & Stover, C. K. Molecular analysis of genetic differences between Mycobacterium bovis BCG and virulent M. bovis. J. Bacteriol. 178, 1274–1282 (1996).

53. Brodin, P. et al. Bacterial Artificial Chromosome-Based Comparative Genomic Analysis Identifies Mycobacterium microti as a Natural ESAT-6 Deletion Mutant. Infect. Immun. 70, 5568–5578 (2002).

54. Abdallah, A. M. et al. Type VII secretion–mycobacteria show the way. Nat. Rev. Microbiol. 5, 883–891 (2007).

55. Bottai, D., Gröschel, M. I. & Brosch, R. Type VII Secretion Systems in Gram-Positive Bacteria. in Protein and Sugar Export and Assembly in Gram-positive Bacteria (eds. Bagnoli, F. & Rappuoli, R.) 404, 235–265 (Springer International Publishing, 2017).

56. Conrad, W. H. et al. Mycobacterial ESX-1 secretion system mediates host cell lysis through bacterium contact-dependent gross membrane disruptions. Proceedings of the National Academy of Sciences 114, 1371–1376 (2017).

57. Majlessi, L. & Brosch, R. Mycobacterium tuberculosis Meets the Cytosol: The Role of cGAS in Anti-mycobacterial Immunity. Cell Host Microbe 17, 733–735 (2015).

58. Fremond, C. M. et al. IL-1 Receptor-Mediated Signal Is an Essential Component of MyD88-Dependent Innate Response to Mycobacterium tuberculosis Infection. The Journal of Immunology 179, 1178–1189 (2007).

59. Muruve, D. A. et al. The inflammasome recognizes cytosolic microbial and host DNA and triggers an innate immune response. Nature 452, 103–107 (2008).

60. Gengenbacher, M. et al. Deletion of nuoG from the Vaccine Candidate Mycobacterium bovis BCG ΔureC::hly Improves Protection against Tuberculosis. MBio 7, (2016).

61. Hornung, V. et al. AIM2 recognizes cytosolic dsDNA and forms a caspase-1-activating inflammasome with ASC. Nature 458, 514–518 (2009).

62. McNab, F., Mayer-Barber, K., Sher, A., Wack, A. & O'Garra, A. Type I interferons in infectious disease. Nat. Rev. Immunol. 15, 87–103 (2015).

63. Berry, M. P. R. et al. An interferon-inducible neutrophil-driven blood transcriptional signature in human tuberculosis. Nature 466, 973–977 (2010).

64. Manca, C. et al. Hypervirulent M. tuberculosis W/Beijing strains upregulate type I IFNs and increase expression of negative regulators of the Jak-Stat pathway. J. Interferon Cytokine Res. 25, 694–701 (2005).

65. Guarda, G. et al. Type I interferon inhibits interleukin-1 production and inflammasome activation. Immunity 34, 213–223 (2011).

66. Novikov, A. et al. Mycobacterium tuberculosis triggers host type I IFN signaling to regulate IL-1β production in human macrophages. J. Immunol. 187, 2540–2547 (2011).

67. Ablasser, A. et al. Cell intrinsic immunity spreads to bystander cells via the intercellular transfer of cGAMP. Nature 503, 530–534 (2013).

68. Orme, I. M., Robinson, R. T. & Cooper, A. M. The balance between protective and pathogenic immune responses in the TB-infected lung. Nat. Immunol. 16, 57–63 (2015).

69. Booty, M. G., Nunes-Alves, C., Carpenter, S. M., Jayaraman, P. & Behar, S. M. Multiple Inflammatory Cytokines Converge To Regulate CD8+ T Cell Expansion and Function during Tuberculosis. J. Immunol. 196, 1822–1831 (2016).

70. Sagoo, P. et al. In vivo imaging of inflammasome activation reveals a subcapsular macrophage burst response that mobilizes innate and adaptive immunity. Nat. Med. 22, 64–71 (2016).

71. Sayes, F. et al. CD4+ T Cells Recognizing PE/PPE Antigens Directly or via Cross Reactivity Are Protective against Pulmonary Mycobacterium tuberculosis Infection. PLoS Pathog. 12, e1005770 (2016).

72. Zhang, L. et al. Variable Virulence and Efficacy of BCG Vaccine Strains in Mice and Correlation With Genome Polymorphisms. Mol. Ther. 24, 398–405 (2016).

73. Ottenhoff, T. H. M. & Kaufmann, S. H. E. Vaccines against tuberculosis: where are we and where do we need to go? PLoS Pathog. (2012).

74. Sayes, F. et al. Multiplexed Quantitation of Intraphagocyte Mycobacterium tuberculosis Secreted Protein Effectors. Cell Rep. 23, 1072–1084 (2018).

3.6 Supplemental figures

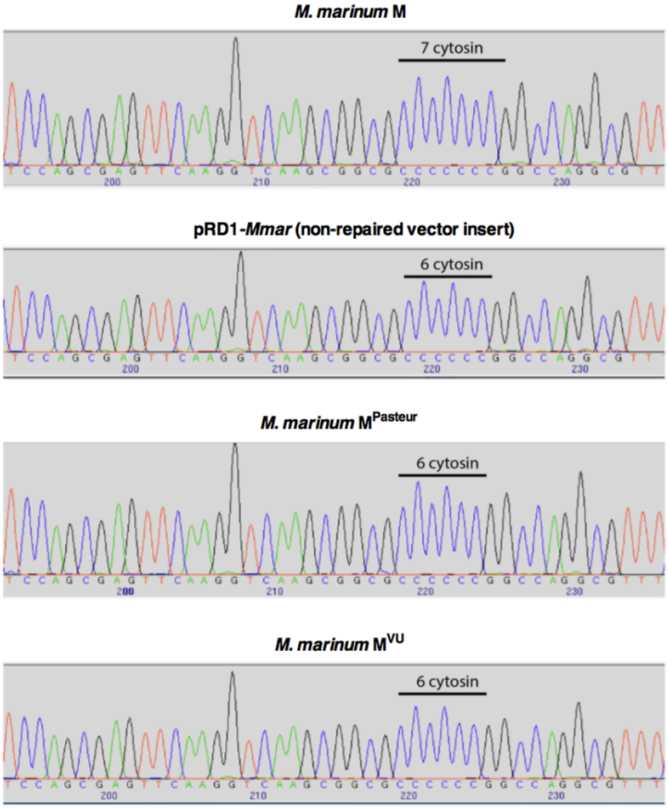

Figure 3.8: **Related to Figure 3.1.** Sequence polymorphisms in the coding region of the *eccCb*$_1$ gene of different *M. marinum* M variants and the original pRD1-*Mmar* cosmid sequence.

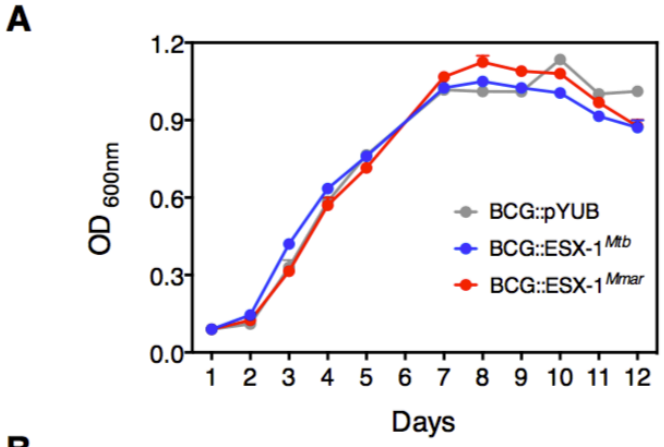

B

ESAT-6 *M. tuberculosis* vs ESAT-6 *M. marinum*

Amino Acid Alignment statistics

Score	Expect	Method	Identities	Positives	Gaps
175 bits(443)	4e-64	Compositional matrix adjust.	87/95(92%)	92/95(96%)	0/95(0%)

```
Query  1   MTEQQWNFAGIEAAASAIQGNVTSIHSLLDEGKQSLTKLAAAWGGSGSEAYQGVQQKWDA  60
           MTEQQWNFAGIEAA+SAIQGNVTSIHSLLDEGKQSL KLAAAWGGSGSEAY+GVQQ WD+
Sbjct  1   MTEQQWNFAGIEAASSAIQGNVTSIHSLLDEGKQSLHKLAAAWGGSGSEAYRGVQQNWDS  60

Query  61  TATELNNALQNLARTISEAGQAMASTEGNVTGMFA  95
           TA ELNN+LQNLARTISEAGQAM+STEGNVTGMFA
Sbjct  61  TAQELNNSLQNLARTISEAGQAMSSTEGNVTGMFA  95
```

CFP-10 *M. tuberculosis* vs CFP-10 *M. marinum*

Amino Acid Alignment statistics

Score	Expect	Method	Identities	Positives	Gaps
191 bits(485)	3e-70	Compositional matrix adjust.	97/100(97%)	98/100(98%)	0/100(0%)

```
Query  1   MAEMKTDAATLAQEAGNFERISGDLKTQIDQVESTAGSLQGQWRGAAGTAAQAAVVRFQE  60
           MAEMKTDAATLAQEAGNFERISGDLKTQIDQVESTAGSLQ QWRGAAGTAAQAAVVRFQE
Sbjct  1   MAEMKTDAATLAQEAGNFERISGDLKTQIDQVESTAGSLQAQWRGAAGTAAQAAVVRFQE  60

Query  61  AANKQKQELDEISTNIRQAGVQYSRADEEQQQALSSQMGF  100
           AANKQK ELDEISTNIRQAGVQYSRAD+EQQQALSSQMGF
Sbjct  61  AANKQKAELDEISTNIRQAGVQYSRADDEQQQALSSQMGF  100
```

Figure 3.9: **Related to Figure 3.1. A.** Comparative growth curve of different recombinant BCG strains in Dubos liquid medium at 37°C. **B.** Protein sequence identities between *M. tuberculosis* and *M. marinum* ESAT-6 or CFP-10, as determined by BLAST.

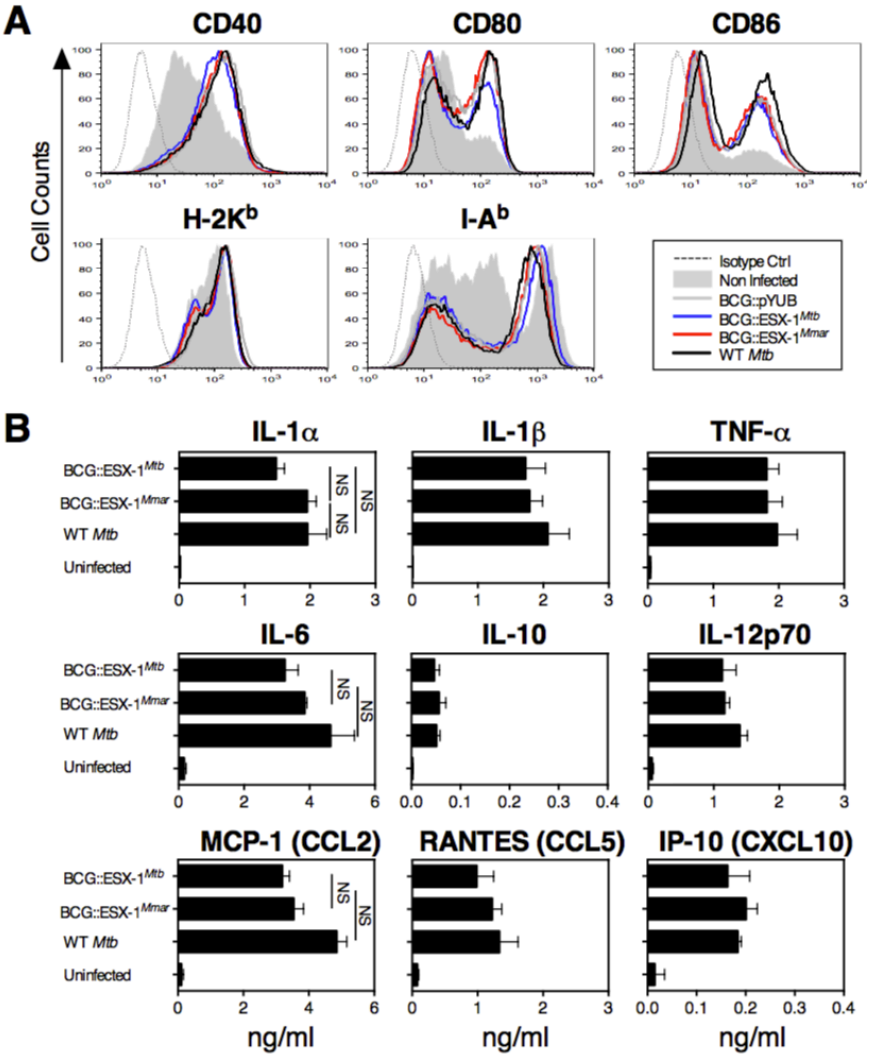

Figure 3.10: *Legend on the following page*

Figure 3.10: Phenotypic and functional activation of innate immune cells induced by BCG::ESX-1 *Mmar*, **Related to Figure 3.3**.

A. Phenotypic maturation of BM-DCs from C57BL/6 mice infected in vitro by different BCG strains (M.O.I. = 1), as judged by cytometric evaluation of surface expression of co-stimulatory or MHC-I or -II molecules at 12h post infection.

B. Functional maturation of the same infected BM- DCs, as determined by pro- or anti-inflammatory cytokine and chemokine quantifications in the supernatants of culture by Multiplexassay. Error bars represent SD. NS = not significant, as determined by One Way ANOVA test with Tukey's correction. The results are representative at least of two independent experiments

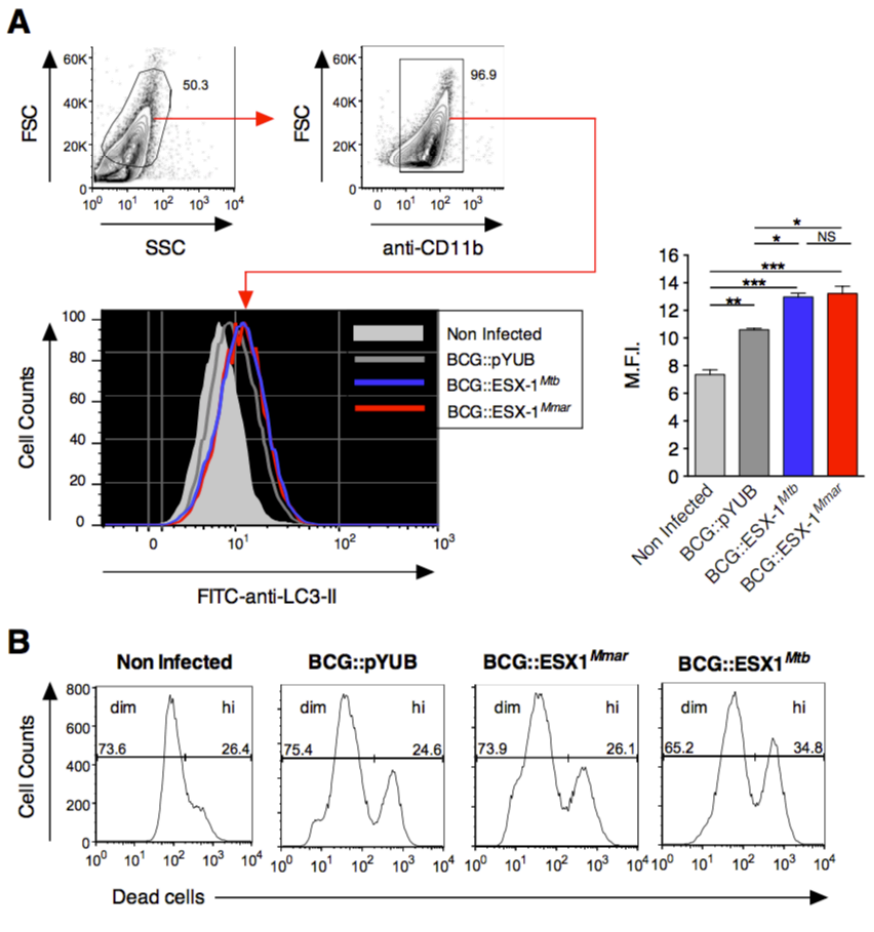

Figure 3.11: *Legend on the following page*

Figure 3.11: **Related to Figure 3.3**.

A. Gating strategy and intensities of intracellular LC3-II expression in THP-1 cells infected with different BCG strains (M.O.I. = 10) at 6h post infection, as evaluated by flow cytometry. NS = not significant, *, ** or *** = statistically significant, as determined by One Way ANOVA test with Tukey's correction, with $p < 0.05$, $p < 0.005$ or $p < 0.001$, respectively.

B. Parallel evaluation of the viability of THP-1 cells, in the same culture wells. Proportions of live (dim) and dead (hi) cells within the $CD11b^+$ population are evaluated by Live/Dead (Invitrogen) staining. The results are representative of two independent experiments.

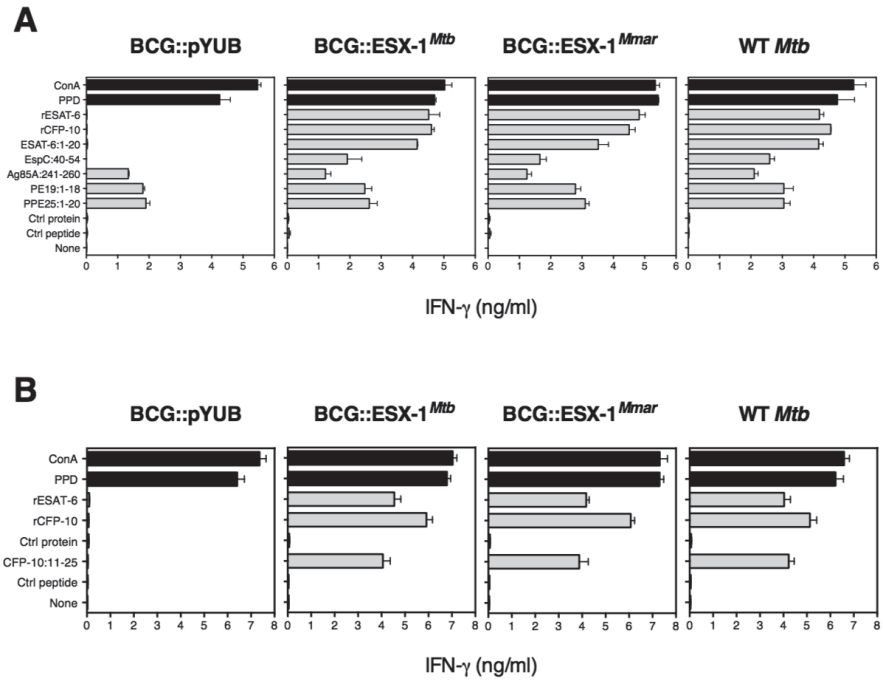

Figure 3.12: T-cell immunogenicity of BCG::ESX-1 *Mmar* in immunocompetent C57BL/6 (H-2^b) and C3H (H-2^k) mice, **Related to Figure 4**.

T-cell IFN-γ responses of C57BL/6 **(A)** or C3H mice **(B)** (n = 3 per group) immunised s.c. with 1 x 10^6 CFU/mouse of different mycobacterial strains, as assessed at 4 wks post-immunisation. Total splenocytes of the immunised mice were stimulated in vitro with different mycobacterial antigens during 72h. Concanavalin A and Purified Protein Derivative (PPD) were used as positive control while rMalE protein and MalE:100-114 peptide were used as negative controls. Error bars represent SD. The results are representative at least of two independent experiments

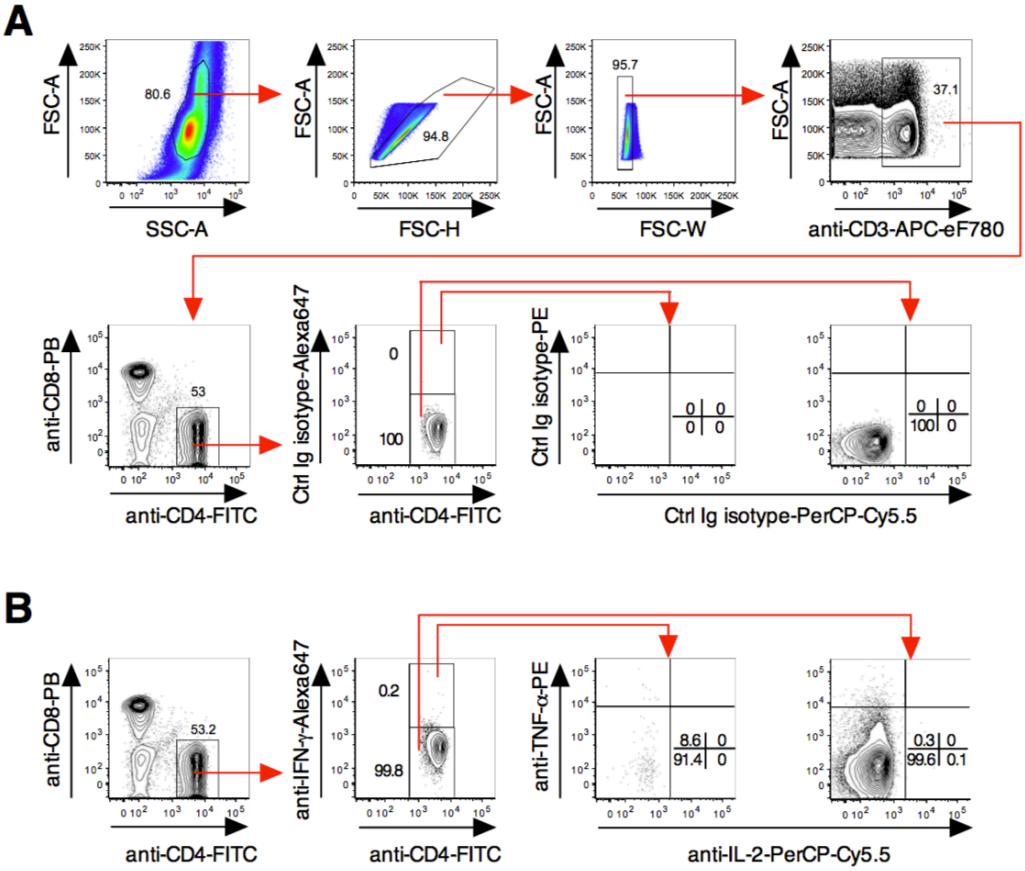

Figure 3.13: Negative controls for ICS assay performed to dissect Th1 subsets in the spleen of BCG::ESX-1 Mmar-immunised mice, **Related to Figure 3.4**.

Gating strategy and cytometric analyses to identify different subsets of Th1 effectors in the splenocytes of BCG::ESX-1 Mmar-immunised C57BL/6 mice stimulated in vitro with 10 μg/ml of PPE25:1-20 peptide and stained with control Ig isotypes **(A)** or stimulated with 10 μg/ml of the MalE: 100-114 negative control peptide and stained with cytokine-specific mAbs **(B)**. Cytometric plots represent 5% contours with outliers, representative of 3 mice per group.

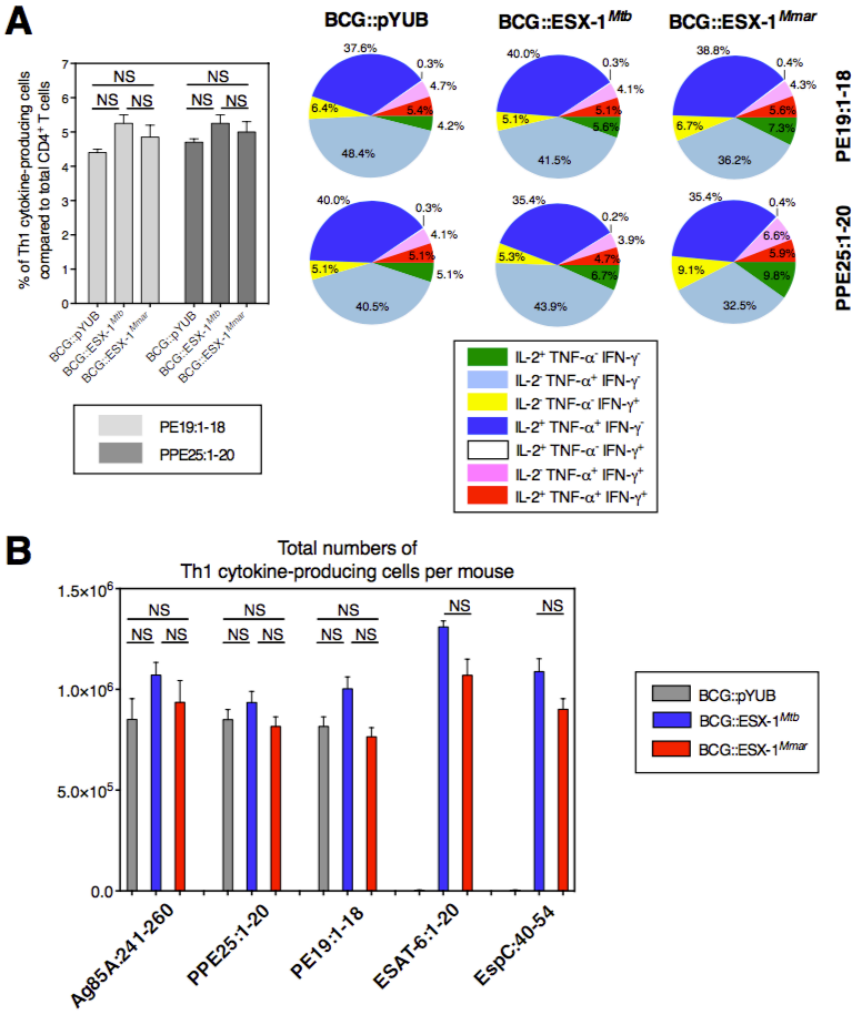

Figure 3.14: *Legend on the following page*

Figure 3.14: Th1-cell responses against PE/PPE proteins induced by BCG::ESX-1 *Mmar* immunisation, **Related to Figure 3.4**.

A. Profile of Th1 cytokine-producing $CD4^+$ T cells, specific to ESX-5-associated PE19 or PPE25 mycobacterial antigens, in the spleen of C57BL/6 mice (n = 3 per group) at 28 days post immunisation with 1 x 10^6 CFU/mouse of different BCG strains. Total splenocytes from each group were stimulated in vitro with 10 μg/ ml of PE19:1-18 or PPE25:1-20 synthetic peptide containing I-A^b-restricted immunodominant epitopes, prior to ICS in order to determine frequencies of single, double or triple IL-2, TNF-α and IFN-γ cytokine-producing $CD4^+$ T cells.

B. Absolute numbers of total Th1 cytokine- producing effector cells in the spleen of the same immunised mice described in Fig 4 and Fig 3.13. These absolute numbers of Th1 effectors specific to individual antigen were calculated for each group based on their percentage obtained from ICS by flow cytometric analyses. Error bars represent SD. NS = not significant, as determined by One Way ANOVA test with Tukey's correction.